

# Behavior of DT-joints in CHS stainless steel tubes including the effect of tensile chord force

Mohamed Mahmoud El-Heweity

Structure Eng. Dept., Faculty of Eng., Alexandria University, Alexandria (21544), Egypt

In this paper, the behavior of welded stainless steel DT-joints fabricated from Circular Hollow Sections (CHS) has been studied numerically. A three dimensional model is done to simulate the behavior of the analyzed joints using the powerful software package COSMOS/M. The model includes both the geometrical and material non-linearity. In the research work done, the joints are firstly analyzed under brace compressive force only in order to determine both the ultimate and service loads. The results are compared with the experimental results available in the literature. Secondly, the effect of the chord tensile forces on the static behavior (the ultimate load, the service load and the mode of failure) of CHS DT-joints is studied. The tensile chord forces are taken as a ratio from the brace compressive force with four load ratios considered in the analysis. The results are plotted in the form of load deformation curves for the analyzed joints under the prescribed load ratios to show how the failure mode of the joint could be changed under the presence of the chord tensile force. Finally, the results of the proposed model are compared with the results of the design formulae (CIDECT and API) of steel CHS. In order to apply the design formulae of carbon steel to stainless steel material, the material constants for carbon steel (i.e. the yield stress) are changed by their equivalents for stainless steel (i.e. the proof stresses). From the comparison done, modification in the API design formula is done to match the results obtained for CHS DT-joints.

فى هذا البحث، تم دراسة سلوك وصلات الاستانلس ستيل الملحومة على شكل DT مصنوعة من مقاطعات دائرية مفرغة. تم عمل نموذج ثلاثى الأبعاد لتمثيل الوصلة باستخدام برنامج COSMOS/M. ويأخذ النموذج فى الاعتبار كلا من لاختية المادة واللاختية الهندسية (لاختية الشكل). تم فى هذا البحث، تحليل الوصلات أولاً تحت تأثير قوة ضاغطة فى العضو الراسى للوصلة وذلك لحساب كلا من الحمل الحدى وحمل الخدمة. تم مقارنة النتائج التى تم الحصول عليها مع النتائج المعملية التى تمت فى استراليا. ثانياً، تم دراسة تأثير وجود قوة الشد الوترية على السلوك الاستاتيكي للوصلة المحللة. تم اعتبار قوة الشد الوترية على انها نسبة من الحمل الراسى المؤثر على الوصلة وتم اعتبار أربعة نسب فى التحليل. تم عرض النتائج على شكل منحنيات الحمل-الازاحة للوصلات المحللة تحت تأثير الأحمال المذكورة لبيان مدى تأثير أشكال الأنهيار للوصلة بوجود أحمال الشد الوترية. أخيراً، تم مقارنة نتائج النموذج المقترح مع نتائج المعادلات التصميمية (CIDECT , API) للمقاطع الحديدية الدائرية المفرغة. ولكى يتم تطبيق هذه المعادلات على مادة الاستانلس ستيل تم استبدال ثوابت المادة للحديد (اجهاد الخضوع) بنظرائها من الاستانلس ستيل. من المقارنة السابقة، تم تعديل المعادلة التصميمية (API) لتواكب النتائج التى تم الحصول عليها.

**Keywords:** Stainless steel, Circular hollow sections, DT-joints, Ultimate capacity, Chord tensile force

## 1. Introduction

Extensive research was performed on welded connections of carbon steel Square Hollow Sections (SHS) and Circular Hollow Sections (CHS) during the last four decades. The research was described in detail in Section 6 of [1] and compiled in a publication by CIDECT [2] and in monographs by Wardenier [3] and Packer and Henderson [4]. The design guidelines, described in these publications, were adopted in the International Institute of Welding (IIW) document [5,6].

In the last decade, cold-formed stainless steel tubular sections are being used increasingly for structural purposes. Typical applications include frameworks in corrosive environments and 2D and 3D truss girders in atriums, canopies, and other roof structures featuring the aesthetic appeal of stainless steel. To facilitate the use of stainless steel tubes in buildings, design guidelines were prepared for the bending and compression strengths of stainless steel square and circular hollow sections [7,8]. These guidelines complemented the specification for the design

of cold-formed stainless steel structural members [9], which is based mainly on tests of light gauge open sections.

The manufacturing process of stainless steel hollow section involves cold-forming a coil strip into a circular shape, welding it, and subsequently sizing it into the desired shape. It is well known that the plastic deformations induced by this process enhance the material properties. This phenomenon is particularly important for austenitic stainless steel tubes because of the pronounced strain-hardening capacity of the material. For carbon steel tubular joints, the CIDECT recommendations [1] permit use of this enhancement by allowing the yield and tensile strengths to be obtained from the finished product rather than the coil strip. Furthermore, it was shown in [7,8] that the bending and compression strengths of stainless steel tubes can be based on the enhanced properties and that the design strengths become very conservative when based on properties of the annealed material. Consequently, the proposed analysis in this paper is based on the properties of the finished product.

A further development in the research of stainless steel tubular sections is developed experimentally by Rasmussen et al. The research concerns the strength of welded X- and K-joints of square and circular hollow sections [10] and [11], respectively. In this research work, tests are described on welded X- and K-joints in SHS and CHS cold-rolled from austenitic 304L stainless steel. The test strengths are compared with design strengths based on the CIDECT recommendations for carbon steel joints [2]. From the experimental results obtained, the design guidelines proposed in this research work adopt the CIDECT recommendations and incorporate the material properties specific to stainless steel.

## 2. Objective of the study

An analytical three-dimensional model for stainless steel in CHS DT-joint has been developed in order to evaluate the static behavior of the joint under compression brace force only and compression brace force with chord tensile force. The proposed model takes into account the effect of the over-all-bending

and the in-plane action in the chord member, the size of weld, and the material and the geometrical non-linearity.

The objective of study in this research work is summarized in the following:

1. A three-dimensional model using the finite element method is presented to evaluate the behavior of DT-joints in CHS stainless steel tubes using the software package COSMOS/M (V 2.6) [12].
2. A parametric study is done to check on the validity of the program COSMOS/M to calculate the ultimate and the service loads of the joint, 3 joints have been analyzed in order to compare between the numerical results obtained and the experimental work done by [11].
3. A new study is done to investigate the effect of the chord tensile force acting in the joint on the ultimate and the service loads of the joints. In this study, the tensile chord force is taken as a ratio from the brace compressive force with four load ratios considered in the analysis. Also, the effect of chord axial force on changing the failure mode and the deformation capacity of the joint is studied for different geometrical parameters of the joints.
4. A design formula for stainless steel CHS joints is given by modifying the American Petroleum Institute design formula [13] to match the results of stainless steel CHS DT-joints.

## 3. The model

In order to carry out this research, the finite element program COSMOS/M (V 2.6 (2000)) [12] is employed. The features of modeling the DT-joint by this program are summarized as follows:

- The behavior of the joint is simulated by three-dimensional model, fig. 1.
- A 4-noded thick shell element is used. In this type of element, each node has three translational and two rotational degrees of freedom. Bilinear interpolation is used for the coordinates, displacements and rotations. For elaborating the element stiffness matrix, seven Simpson integration layers are used in the thickness direction of the elements, and 2×2 Gaussian integration points are used in each

layer of the elements. It should be mentioned that the reduced integration method is not needed because the contribution of the bilinear displacement and rotation field to the strain energy is a second order polynomial for which the 2x2 Gaussian integration points are enough for the exact solution.

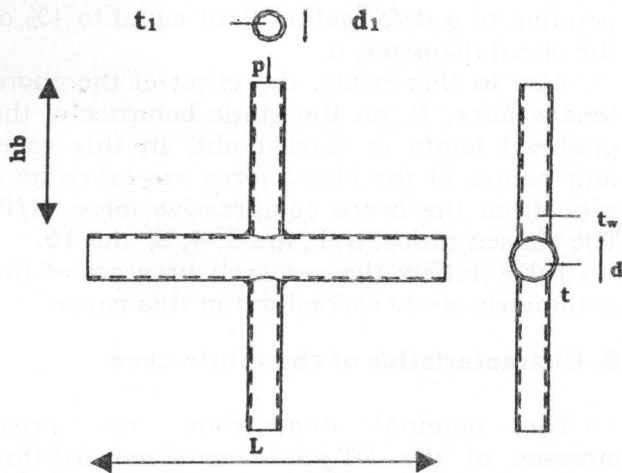


Fig. 1 Definition of symbols (shape of the joint).

- The ends of the chord member of the analyzed joint are assumed to deform freely while the brace members are constrained to move vertically only.

The loads are applied in an incremental manner using the modified Newton-Raphson technique. The Arc-length method is used to

pass the limit point and to trace the behavior of the joints in the post-plastic stage.

- The displacement convergence criterion is used with convergence tolerance equals 1 mm.

- To account for the material nonlinearity, material curve description is used. Fig. 2 shows the material curve describing the stress-strain relation of stainless steel material.

- In order to describe the large displacement problem, the total Lagrangian procedure is used.

- To introduce the size of weld in the joint, the fillet weld is taken as a shell element with an average thickness  $t_w$ . The average thickness  $t_w$  was recommended by [14] and is given by eq. (1):

$$t_w = \frac{a_v \times a_h}{2l_w}, \quad (1)$$

where,  $a_v$  and  $a_h$  are the vertical and the horizontal legs of the weld respectively and  $l_w$  is the inclined length of the weld.

- The vertical brace force and the chord tensile forces are assumed to be distributed uniformly along the brace and chord cross sections respectively as shown in fig. 3. This is done by adding thick plates at the ends of both the chord and the brace members to allow the suggested transfer of the load.

Fig. 4. shows the finite element mesh for quarter of the analyzed joint.

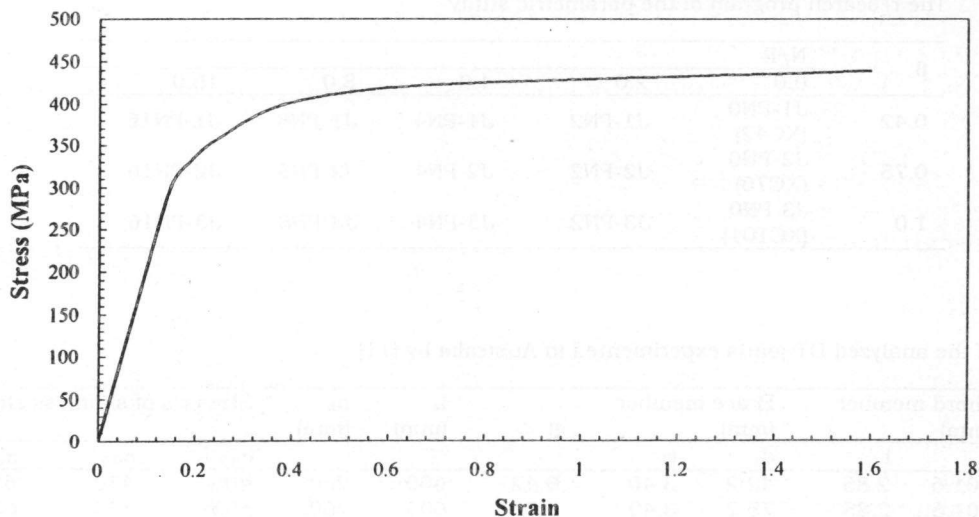


Fig. 2. Stress-strain curve of stainless steel material.

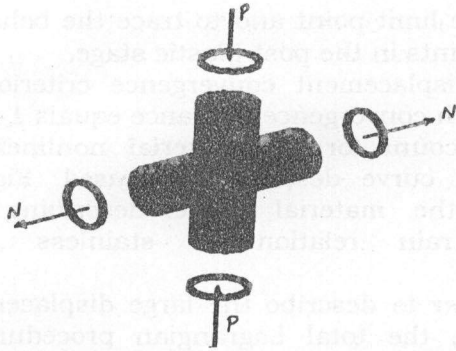


Fig. 3. Distribution of forces on the analyzed joint.

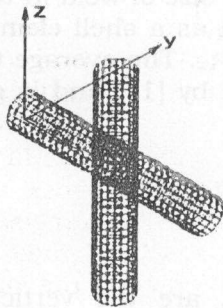


Fig. 4. Finite element mesh of the analyzed joint.

**4. Parametric study**

In this study, 3 joints experimented in Australia by Rasmussen and Hasham (2001) have been analyzed under axial force, P, acted through the brace member of the joint. The

brace ratios  $\beta$  of brace diameter to chord diameter are varied by 0.42, 0.76, and 1.0 respectively. The ultimate loads of the DT-joints have been calculated and compared with the experimental results. The maximum horizontal and vertical deflections of the joint are plotted with the applied load P. For each joint, the service load is calculated corresponding to a deformation limit equal to 1% of the chord diameter, d.

Also in this study, the effect of the chord tensile force, N, on the static behavior of the analyzed joints is carried out. In this case, four values of the chord force are taken as a ratio from the brace compressive force, N/P. The chosen ratios, N/P, are 2, 4, 8, and 16.

Table 1 lists the research program of the parametric study carried out in this paper.

**5. Characteristics of the joints used**

The nominal dimensions, the proof stresses of the DT-joints analyzed in this study are tabulated in table 2. The table includes for each joint: the dimensions of both the chord and the brace members; the ratio of the diameter of the brace to that of the chord,  $\beta$ ; the length of the chord member, L; the height of the brace member,  $h_b$ ; the measured 0.2 and 0.5% proof stresses and the ultimate stress of the stainless steel material.

Table 1  
The research program of the parametric study

$\beta$	N/P				
	0.0	2.0	4.0	8.0	16.0
0.42	J1-PN0 (XC42)	J1-PN2	J1-PN4	J1-PN8	J1-PN16
0.75	J2-PN0 (XC76)	J2-PN2	J2-PN4	J2-PN8	J2-PN16
1.0	J3-PN0 (XC101)	J3-PN2	J3-PN4	J3-PN8	J3-PN16

Table 2  
Dimensions of the analyzed DT-joints experimented in Australia by [11]

Joint	chord member (mm)		Brace member (mm)		$\beta$	L (mm)	$h_b$ (mm)	Stresses of stainless steel (MPa)		
	d	t	$d_1$	$t_1$				$\sigma_{0.2}$	$\sigma_{0.5}$	$\sigma_u$
	XC42	101.6	2.85	42.2				3.40	0.42	600
XC76	101.6	2.85	76.2	3.40	0.76	600	260	405	430	630
XC101	101.6	2.85	101.6	2.85	1.00	600	260	405	430	630

## 6. Numerical results

The results are listed in tables 3 and 4 for the analyzed DT-joints. Table 3 shows the ultimate and service Loads (corresponding to deflection equals 1%*d*) resulted from both the proposed model and the experimental work done by [11]. In table 4, the ultimate and service Loads,  $P_{un}$  and  $P_{sn}$ , respectively (the suffix *n* is used in case of combined brace compressive force and chord tensile force) resulted from the proposed model in case of chord tensile forces are presented. In the following subsections the numerical results obtained are discussed.

Table 3  
Comparison between the results of the proposed model and the experimental results done by [11]

Joint	Ultimate load (kN)		Service load(kN)	
	$(P_u)_{model}$	$(P_u)_{exp}$	$(P_s)_{model}$	$(P_s)_{exp}$
XC42	31.3	35.2	14.2	16.3
XC76	53.8	60.2	30.3	36.2
XC101	142.4	152.0	120.1	127.2

### 6.1. Verification of the proposed model

Figs. 5-a and 5-b show the compressive brace force,  $P$ , versus the vertical and the sidewall (horizontal) deflections of the joints, respectively for the analyzed and experimented

joints. The sidewall deflection is defined as the maximum horizontal deflection at the center of the joint.

From the results given in table 3, it can be seen that the numerical results obtained by using the proposed model have a good agreement with those obtained experimentally in Australia by [11]. The ultimate and service loads of the joints are lower than the experimental results by about 9.5% and 11.5%, respectively.

From figs. 5-a and 5-b, good agreement with the experimental results is proved. Also, one can notice that the failure of the joints in case of the proposed model occurs in a stage earlier than the experimental ones. This is because the failure of the joint in case of the theoretical model is defined as the load which gives the first ultimate stress on the joint while in the experimental analysis the failure of the joint occurs when much number of plastic hinges are formed in the joint.

### 6.2. Effect of chord tensile force on the service load and the ultimate load of the joints

From table 4 and fig. 6, some important conclusions can be observed:

1. Generally for DT-joints having different diameter ratio,  $\beta$ , the service load and the ultimate load of the joint decrease by increasing the chord tensile force,  $N$ .

Table 4  
Numerical results of DT-joints in case of tensile chord force

Joint	$\beta$	$N/P$	Ultimate load ( $P_{un}$ ) (kN)	Service load ( $P_{sn}$ ) (kN)	$P_{un}/P_u$	$P_{sn}/P_s$
Joint 1	0.42	0.0	31.3	14.2	1.0000	1.0000
		2.0	33.47	14.25	1.0692	1.0038
		4.0	33.82	14.51	1.0805	1.0220
		8.0	30.14	14.08	0.9628	0.9915
		16.0	21.38	12.52	0.6831	0.8815
Joint 2	0.76	0.0	53.8	30.3	1.0000	1.0000
		2.0	49.59	29.74	0.9217	0.9816
		4.0	47.71	28.26	0.8868	0.9325
		8.0	40.97	25.39	0.7615	0.8381
		16.0	25.54	20.10	0.4747	0.6632
Joint 3	1.00	0.0	142.4	120.10	1.0000	1.0000
		2.0	103.5	99.25	0.7268	0.8264
		4.0	83.06	74.09	0.5833	0.6169
		8.0	54.71	47.16	0.3842	0.3927
		16.0	34.35	32.30	0.2412	0.2689

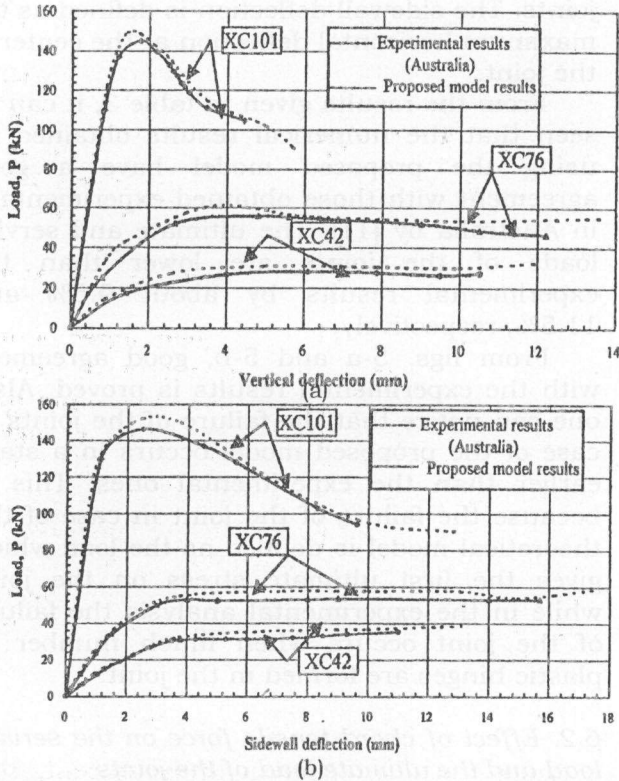


Fig. 5. Load versus deformation curves for the analyzed and experimented DT-joints under compressive brace force.

2. For  $\beta=1.0$ , the service load and the ultimate load of the analyzed joints decrease rapidly till the ratio  $N/P \approx 6$ . For  $N/P$  higher than 6 the value of these loads decrease gradually.
3. For joints of  $\beta \leq 0.50$ , the effect of the chord force on the service load and the ultimate load of the joints is very small and can be neglected till the ratio  $N/P=8$ . For  $N/P > 8$ , the effect of the chord tensile force must be taken into account.
4. For moderate diameter ratio,  $0.5 < \beta < 0.8$ , the tensile chord force reduces the ultimate loads by about 11%, 24% and 53% for ratios  $N/P=4, 8$  and  $16$ , respectively.

### 6.3. Effect of chord tensile force on the failure mode of the joints

The effect of the tensile chord force on changing the failure mode of the joints is discussed briefly for different load ratios,  $N/P$ , and for different sets of diameter ratio,  $\beta$ . The load deformation curves of the analyzed joints are plotted in figs. 7 (a, b, and c). From these

figures, the following conclusions may be found:

1. The failure of joints having diameter ratio,  $\beta \leq 0.75$  is associated with large deformations of the chord. This is verified as shown in the figures.

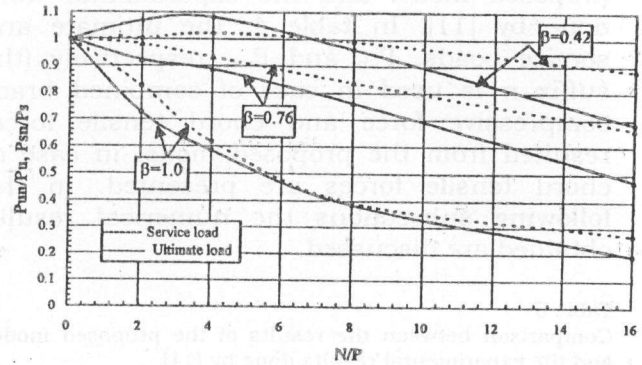


Fig. 6. Effect of tensile chord force on the ultimate and service loads of the analyzed joints.

2. The load deformation curves of the joints having width ratio,  $\beta \leq 0.75$  have not affected by the chord tensile force till the ratio  $N/P$  reaches 8. For joints having load ratio equals to or greater than 8, the load deformation curves drift but still having the same failure mode.
3. The failure mode of joints having diameter ratio,  $\beta=1.0$  is crippling failure. This is verified as shown in the figures.
4. The load deformation curves of the joints having diameter ratio,  $\beta=1.0$  are affected by the chord tensile force till the ratio  $N/P$  reaches 4 with crippling mode of failure. For joints having load ratio greater than 4, the mode of failure changes from crippling failure mode to chord failure mode.

## 7. Design formula

### 7.1. Introduction

In the absence of a distinct yield stress of stainless steel, the approach adopted in the Specification for the design of cold-formed stainless steel structural members [9] is to use strength equations derived for carbon steel cold-formed members. This approach was done by replacing the material constants for carbon steel and inserting their equivalents for

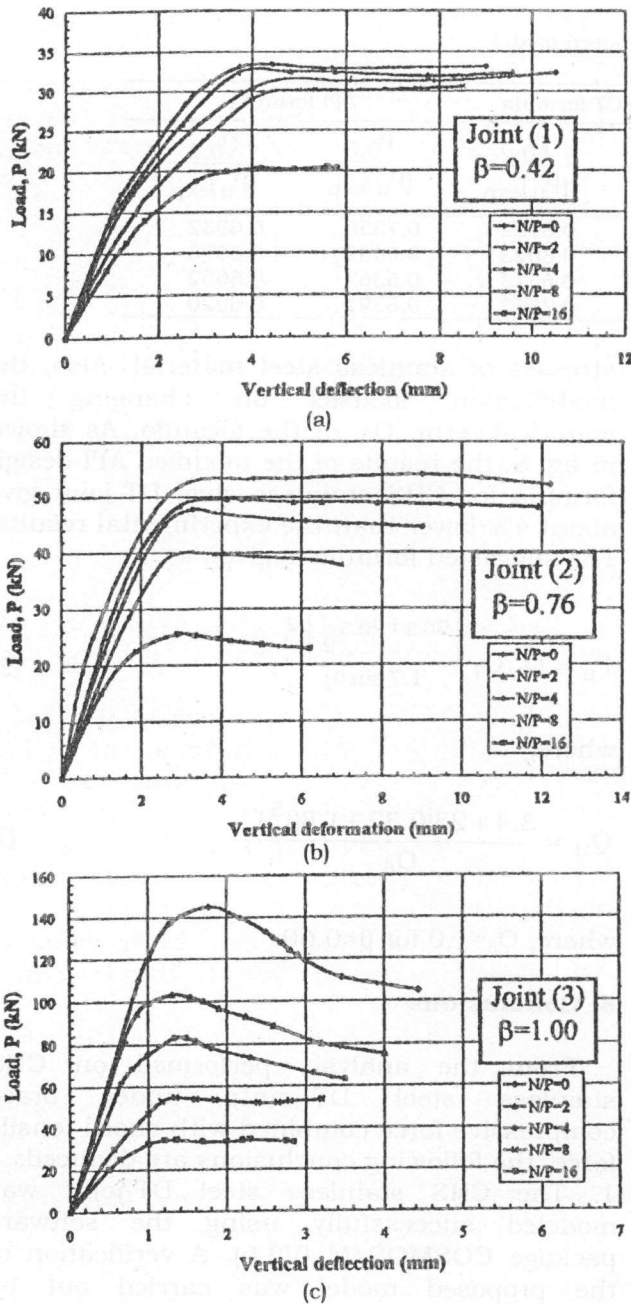


Fig. 7. Load versus deflection for the analyzed DT-joints in case of chord tensile force.

stainless steel. The same approach was extended to CHS welded joints in the research work done by [11] by adopting the CIDECT [2] strength equations, which are also included in Annex 'K' of Eurocode 3 [6] and endorsed by the International Institute of Welding [5] and replacing the yield stress of carbon steel by

the proof stress of stainless steel in these equations.

In this paper, the same technique is used by adopting the API design formula [13] and replacing the yield stress of carbon steel by the proof stress of stainless steel obtained experimentally by [11] in these equations.

In the API design formula [13], the allowable nominal brace load,  $P_a$ , for DT-joints under balanced compressive force is defined as:

$$P_a = Q_u Q_f \frac{\sigma_y t^2}{1.7 \sin \theta_1} \quad (2)$$

For DT-joints,  $\sin \theta_1 = 1.0$ . The 1.7 dominator is termed the joint safety factor and the ultimate strength factor  $Q_u$  is quoted as:

$$Q_u = \frac{3.4 + 13\beta}{Q_\beta} \quad (3)$$

where,  $Q_\beta = 1.0$  for  $\beta < 0.60$ .

When nominal chord load is present, the chord stress factor  $Q_f$  needs to be taken into account. For axial chord stress,  $Q_f$  is given as:

$$Q_f = 1 - \omega(2\gamma)A^2 \quad (4)$$

The value of the  $\omega$  factor is dependent on the type of brace load and for axial load,  $\omega = 0.03$ . The 'A' term is referred to as the chord utilization ratio and it can be defined as:

$$A = \frac{\sigma_{ax}}{0.6\sigma_y} \quad (5)$$

where,  $\sigma_{ax}$  = chord nominal axial stress and the 0.60 dominator is the chord stress safety factor.

### 7.2. Comparison between design formulae and the proposed model

The ultimate loads of the analyzed DT-joints are compared with those determined using the CIDECT design formula [1] and the API design formula [13]. The comparisons are given in table 5 in the form of ratios between

Table 5  
Comparison between design formulae and the proposed model.

Joint	$\beta$	$\frac{P_{un}}{(P_u)_{exp}}$	CIDECT formula		API formula	
			$\frac{P_{0.5}}{(P_u)_{exp}}$	$\frac{P_{0.2}}{(P_u)_{exp}}$	$\frac{P_{0.5}}{(P_u)_{exp}}$	$\frac{P_{0.2}}{(P_u)_{exp}}$
Joint 1	0.42	0.8892	0.8693	0.8182	0.7358	0.6932
Joint 2	0.76	0.8937	0.8522	0.8023	0.6452	0.6076
Joint 3	1.00	0.9368	0.6908	0.6513	0.5362	0.5052
Mean		0.9066	0.8041	0.7573	0.6391	0.6020

the evaluated loads and the experimental ones. From the table and fig. 8, it can be seen that the results obtained by the proposed model have a good agreement with the experimental results. Also, The CIDECT design formula is about 25% and 20% lower than the experimental results when replacing the yield stress by the 0.2 and 0.5% proof stress respectively. The API design formula is conservative when replacing the yield stress of steel by the proof stress of stainless steel, it gives 36% and 40% lower than the experimental results for 0.5 and 0.2% proof stress, respectively.

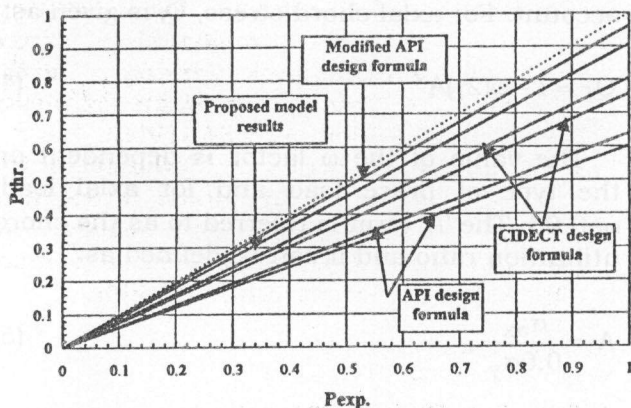


Fig. 8. Comparison between the design formulae and the proposed model results.

### 7.3. Modified API design formula

From the results obtained in the previous section, the API design formula looks very conservative comparing with the experimental and the theoretical results. A trial to modify the API design formula is carried out. The modification depends on replacing the yield stress of carbon steel in the API formula by the average of the 0.2% and 0.5% proof

stresses of stainless steel material. Also, the modification focuses on changing the empirical term,  $Q_u$ , of the formula. As shown in fig. 8, the results of the modified API design formula for CHS stainless steel DT-joint give about 4% lower than the experimental results. The suggested formula is given as:

$$P_a = Q_u Q_f \left[ \frac{\sigma_{0.2} + \sigma_{0.5}}{2} \right] t^2, \quad (6)$$

where,

$$Q_u = \frac{3.4 + 23(0.32 + 1.8\beta^5)}{Q_\beta}, \quad (7)$$

where,  $Q_\beta = 1.0$  for  $\beta < 0.60$ .

## 8. Conclusions

From the analysis performed on CHS stainless steel DT-joints under brace compressive force combined with chord tensile force, the following conclusions are deduced:

1. The CHS stainless steel DT-joint was modeled successfully using the software package COSMOS/M (V2.6). A verification of the proposed model was carried out by comparing the proposed model results with the experimented results in Australia.
2. The chord tensile force acting on the joint must be considered in the local analysis of the joint. The importance of the chord force differs from one joint to another depending on the value of the chord force and the geometrical parameters of the joint.
3. A modification in the API design formula is carried out to calculate the ultimate load of stainless steel CHS DT-joints. The modified



formula calculates the ultimate load of the joint by about 4% lower than the experimental results.

## References

- [1] Comité International pour le Développement et l'Étude de la Construction Tubulaire (CIDECT). The strength and behaviour of statically loaded welded connections in structural hollow sections, Monograph No. 6, British Steel Corporation, London (1986).
- [2] J., Wardenier, Y., Kurobane, J. Packer, A., Dutta, D., and Yeomans, N. Design Guide for Circular Hollow Section (CHS) Joints under Predominantly Static Loading, Comité International pour le Développement et l'Étude de la Construction Tubulaire (CIDECT), Verlag TUV Rheinland GmbH, Cologne, Germany (1991).
- [3] J. Wardenier, Hollow section joints, Delft University Press, Delft, The Netherlands (1982).
- [4] J. A., Packer, J. E. and Henderson, Hollow structural section connections and trusses: A design guide, 2<sup>nd</sup> Ed., Canadian Institute of Steel Construction, Ontario, Canada (1997).
- [5] International Institute of Welding (IIW). Design recommendation for hollow section joints: Predominantly statically loaded, 2<sup>nd</sup> Ed., IIW Document XV-701-89, Cambridge, U.K. (1989).
- [6] Commission of the European Communities (CEN). Common unified rules for steel structures, Part 1.1." Eurocode 3, Brussels (1992).
- [7] K.J.R. Rasmussen, and G. J. Hancock, "Design of cold formed stainless steel tubular members. I: Columns" Journal of structural Engineering, ASCE, Vol. 119 (8), pp. 2349-2367 (1993).
- [8] K.J.R. Rasmussen, and G.J. Hancock, "Design of cold formed stainless steel Tubular members. II: Beams." Journal of structural Engineering, ASCE, Vol. 119 (8), pp. 2368-2386 (1993).
- [9] American society of civil Engineering (ASCE). "Specification for the design of cold-formed stainless steel structural members". New York (1991).
- [10] K.J.R. Rasmussen, B. Young, "Tests of X- and K-Joints in SHS stainless Tubes." J. Struct. Engrg., ASCE, Vol. 127(10), pp. 1173-1182 (2001).
- [11] K. J. R., Rasmussen, A. and Hasham, "Tests of X- and K-joints in CHS stainless steel tubes." J. Struct. Engrg., ASCE, Vol. 127(10), pp.1183-1189 (2001).
- [12] Cosmos/M version 2.6, "A computer program for nonlinear static and dynamic analysis", structural Research and Analysis Corporation, Santa Monica, California, USA (2000).
- [13] API Recommended Practice 2A-WSD, Recommended Practice for Planning, Designing, and Constructing Fixed Offshore Platforms-Working stress design, 20<sup>th</sup>. Edition, American Petroleum Institute, Washington, USA (1993).
- [14] Y. Yu and J. Wardenier, "Influence of the Types of Welds on the Static Strength of R.H.S T-and X-Joints Loaded in Compression," Sixth International Symposium on Tubular Structures (1994).

Received October 12, 2002  
Accepted November 23, 2002

industrial steel joists. In Columns, Joists and  
Structural Engineering, ASCE, Vol. 19  
(8), pp. 2349-2357 (1993).

[8] K.J.F. Housheer and G.J. Hartcock,  
Design of cold formed stainless steel  
Tubular members. In Beams, Journal of  
Structural Engineering, ASCE, Vol. 119 (8),  
pp. 2304-2310 (1993).

[9] American Society of Civil Engineering  
(ASCE), Specification for the design of  
cold formed stainless steel structural  
members, New York (1991).

[10] E.A.R. Rasmussen, B. Young, Tests of X  
and K-joints in SHS stainless Tubular J  
Struct. Engng, ASCE, vol. 127(10), pp.  
1154-1162 (2001).

[11] K. R. Rasmussen, A. and Hasham,  
Tests of X and K-joints in CHS stainless  
steel tubes, J. Struct. Engng, ASCE, Vol.  
127(10), pp. 1163-1169 (2001).

[12] Cosmos M, version 5.0, Acumatica  
program for nonlinear static and dynamic  
analysis, structural research and design  
Corporation, Santa Monica, California,  
USA (2000).

[13] AISI Recommended Practice for Design  
and Construction of Cold-Formed Steel  
Members, American Iron and Steel  
Institute, Washington, USA (1993).

[14] Y. Yu and J. Wardenier, Influence of the  
Type of Weld on the Static Strength of  
KHS-1 and X-joints loaded in  
compression, Sixth International Sympo-  
sium on Tubular Structures (1994).

Received August 27, 2003  
Accepted November 21, 2003

results calculated for the most part of the  
joint by about 4% lower than the experimental  
results.

References

[1] Comité International pour le Développement  
et l'Étude de la Construction Tubulaire  
(CIBCT), The strength and behaviour of  
externally loaded welded connections in  
structural hollow sections, Monograph No.  
6, Bureau Euro-Construction, London  
(1982).

[2] J. Wardenier, Y. Kuvshinov, A. Packer, A.  
and J. P. and Youssef, N. Design Guide  
for Tubular Hollow Section (THS) Joints  
under predominantly static loading,  
Comité International pour le  
Développement et l'Étude de la  
Construction Tubulaire (CIBCT), Verlag  
TUB-Technik GmbH, Cologne, Germany  
(1991).

[3] J. Wardenier, Hollow section joints, Delft  
University Press, Delft, The Netherlands  
(1982).

[4] J. A. Packer, J. E. and Henderson, Hollow  
structural section connections and  
trusses, A design guide, 2nd Ed., Canadian  
Institute of Steel Construction, Ontario,  
Canada (2007).

[5] International Institute of Welding (IIW),  
Design recommendation for hollow section  
joints, Proceedings, 2nd Int. Conf. on  
ECB, IIW Document XV-701-89,  
Cambridge, U.K. (1989).

[6] Commission of the European Communities  
CEC, Common unified code for steel  
structures, Part 1.1, Eurocode 3,  
Brussels (1992).

[7] A. R. Rasmussen and G. J. Hartcock,  
Design of cold formed stainless steel